Zhong Yin, Ivan Rajkovic, Sreevidya Thekku Veedu, Sascha Deinert, Dirk Raiser, Rohit Jain, Hironobu Fukuzawa, Shin-ichi Wada, Wilson Quevedo, Brian Kennedy, Simon Schreck, Annette Pietzsch, Philippe Wernet, Kyoshi Ueda, Alexander Föhlisch, and Simone Techert*

Ionic Solutions Probed by Resonant Inelastic X-ray Scattering

DOI 10.1515/zpch-2015-0610
Received March 31, 2015; accepted July 20, 2015

***Corresponding author: Simone Techert,** Photon Science, Deutsches Elektronen-Synchrotron, 22607 Hamburg, Germany; and Structural Dynamics of (Bio)chemical Systems, Max Planck Institute for Biophysical Chemistry, 37077 Göttingen, Germany; and Institute for X-ray Physics, University of Göttingen, 37077 Göttingen, Germany, e-mail: simone.techert@desy.de
Zhong Yin: Photon Science, Deutsches Elektronen-Synchrotron, 22607 Hamburg, Germany; and Structural Dynamics of (Bio)chemical Systems, Max Planck Institute for Biophysical Chemistry, 37077 Göttingen, Germany
Ivan Rajkovic, Dirk Raiser, Rohit Jain: Structural Dynamics of (Bio)chemical Systems, Max Planck Institute for Biophysical Chemistry, 37077 Göttingen, Germany
Sreevidya Thekku Veedu: Photon Science, Deutsches Elektronen-Synchrotron, 22607 Hamburg, Germany; and Structural Dynamics of (Bio)chemical Systems, Max Planck Institute for Biophysical Chemistry, 37077 Göttingen, Germany
Sascha Deinert: Photon Science, Deutsches Elektronen-Synchrotron, 22607 Hamburg, Germany
Hironobu Fukuzawa, Kyoshi Ueda: Institute of Multidisciplinary Research for Advanced Materials, Tohoku University, Sendai, Japan
Shin-ichi Wada: Department of Physical Science, Hiroshima University, Higashi-Hiroshima 739-8526, Japan
Wilson Quevedo, Brian Kennedy, Annette Pietzsch, Philippe Wernet: Institute for Methods and Instrumentation for Synchrotron Radiation Research, Helmholtz-Zentrum Berlin GmbH, 12489 Berlin, Germany
Alexander Föhlisch: Institute for Methods and Instrumentation for Synchrotron Radiation Research, Helmholtz-Zentrum Berlin GmbH, 12489 Berlin, Germany; and Institut für Physik und Astronomie, Universität Potsdam, 14476 Potsdam, Germany
Simon Schreck: Institute for Methods and Instrumentation for Synchrotron Radiation Research, Helmholtz-Zentrum Berlin GmbH, 12489 Berlin, Germany; and Institut für Physik und Astronomie, Universität Potsdam, 14476 Potsdam, Germany; and present address: Department of Physics, AlbaNova University Center, Stockholm University, 10691, Sweden

Abstract: X-ray spectroscopy is a powerful tool to study the local charge distribution of chemical systems. Together with the liquid jet it becomes possible to probe chemical systems in their natural environment, the liquid phase. In this work, we present X-ray absorption (XA), X-ray emission (XE) and resonant inelastic X-ray scattering (RIXS) data of pure water and various salt solutions and show the possibilities these methods offer to elucidate the nature of ion-water interaction.

Keywords: X-ray Spectroscopy, XAS, XES, RIXS, Anions, Cations, Liquid Jet, Synchrotron Radiation.

Dedicated to Prof. Dr. Dr. h.c. mult. Jürgen Troe on the occasion of his 75th birthday

1 Introduction

The development of third and fourth generations of light sources and the concomitant improvement of beam properties, e.g. brilliance and coherence, enables a broad range of experimental techniques to study samples with atomic resolution. Information about the electronic structure of chemical systems are difficult to obtain due to the characteristic energies of the molecular orbitals, yet they contain necessary information about bonding relations, symmetry or chemical environment to name a few [1, 2]. One of the techniques to monitor the electronic structure is X-ray spectroscopy. While X-ray absorption spectroscopy (XAS) is for monitoring the unoccupied states of an element, X-ray emission spectroscopy (XES) is probing the occupied orbitals. A special case is the so called resonant inelastic X-ray scattering (RIXS).

In XAS, a core electron is excited with a monochromatic X-ray source to an unoccupied molecular orbital or above the ionization threshold to create a vacancy. In soft X-ray emission spectroscopy, the created excited system relaxes via valence electrons filling the core-hole under emission of a photon. Both contain information about the electronic structure of the molecules under investigation. XES is further divided into resonant XES (RIXS) and non-resonant XES. In RIXS, the core electron excitation to an unoccupied state and the following fluorescence are coupled events. The non-resonant XES is a two-step process, where the absorption and the emission are decoupled processes [3, 4]. An illustration of the molecular orbitals of water and the differences between XAS, XES and RIXS are shown in Figure 1. XES is element, orbital and site specific and sensitive to the chemical environment as well as the symmetry. Moreover, photons offer bulk information as

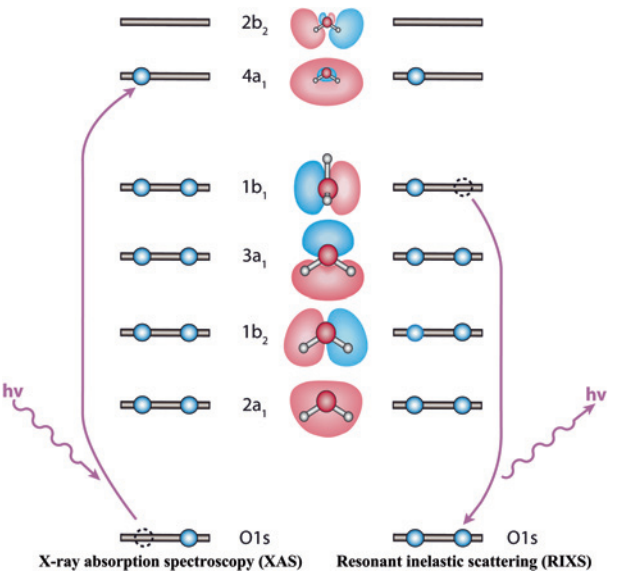

Figure 1: Schematic description of XAS and RIXS with molecular orbitals of water. For non-resonant XES the core electron is excited above the ionization threshold.

the penetration length is much higher compared to electrons. Overall X-ray spectroscopy is an ideal tool to study the local electronic structure [5–23].

Salt-water interaction is ubiquitous in chemical and biochemical processes. The impact of salts even plays an essential role in the metabolism of eukaryotic cells and in the case of mammalians it can lead to critical aggregation effects which were discussed as various pre-stages of diseases [25–27]. A manifold of experiments using different techniques have been applied to shed light to the ion-water interaction [2, 28–37]. Yet, there is an incomplete understanding of salt-water interaction on the molecular level.

In this work we are presenting the possibilities that X-ray spectroscopy offers to elucidate the nature of ion-water interaction, showing the results of salt solutions compared to water with various anions, because it is believed that anions have a stronger contribution to the salt's impact than cations [25]. Additionally, we present a concentration dependent measurements as well as the possibility to probe an element site specifically.

2 Experimental section

The experiments were performed at the beamline U41_PGM and U49/2-PGM1 of the synchrotron radiation source at the Helmholtz Zentrum Berlin using the

FlexRIXS [38] and Transmission NEXAFS [39] endstations and at P04 of PETRA III at DESY site in Hamburg using the ChemRIXS endstation. X-ray absorption measurements in transmission mode were performed with a liquid cell [38]. XES and RIXS experiments were performed with a liquid jet [24, 40]. For excitation, a monochromatic X-ray beam with $\sim 10^{12}$ photons per second on the sample has been utilized. The jet system consists of a mixer, a degasser and an HPLC pump (JASCO). The implementation of the liquid jet provides continuously fresh samples and avoids radiation damage during the experiment. In contrast to a liquid flow cell, the liquid jet also prevents interaction of X-rays and samples with the cell membrane and also prevents further loss of photon flux. Principally, the diameter of the liquid jet can vary from 5–100 μm. For the presented measurements in this article we used a 20 μm jet. Immediately after passing through the nozzle, the liquid has a laminar flow for a certain length. Depending on the sample, flow rate and nozzle diameter is in the range of a few millimeters [41, 42], which is used to probe the system of interests.

The aqueous salt solutions were prepared from commercially available salts of highest purity from Sigma-Aldrich at least 12 h prior to the experiment. The resonant and non-resonant excitation energies have been selected from the X-ray absorption spectra (XAS) of water and aqueous solutions recorded in transmission mode. XA and XE spectra of pure water were recorded periodically to confirm the stability of the setup. The monochromator slit was set to an energy bandwidth of approx. 0.4 eV. The resolution of the grating spectrometer was 0.4 eV at 530 eV (oxygen K-edge). The elastic peaks were used for energy calibration.

3 Experimental results and discussion

Figure 2 shows a RIXS map of water taken at the oxygen K-edge. A RIXS map is a series of X-ray emission measurements around the absorption edge of a sample. Integration of X-ray emission intensities in dependence of the excitation energy results in an X-ray absorption spectrum from partial fluorescence yield [8].

All spectra have been area normalized to provide an accurate comparison of relative intensities. B and C correspond to the bonding orbitals $3a_1$ and $1b_2$ and peak A to the lone pair electrons $1b_1$.

Figure 3 shows the non-resonant X-ray emission spectra of pure water in comparison with various salt solutions at the oxygen edge at an excitation energy of 540 eV. The figure is showing data from 500 mM salt solutions with NH_4^+ as the cation and various different anions compared to pure water as reference. No significant changes are observable in all low concentrated solutions. The XE spectrum

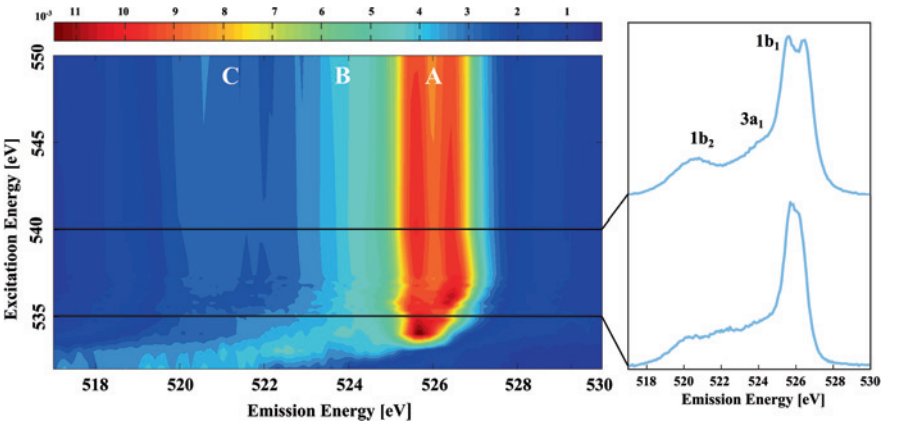

Figure 2: RIXS map of liquid water at the oxygen K-edge shows above an excitation energy of around 537 eV a broader line with a fine structure at A. The right spectra display horizontal cuts of the RIXS map at two different excitation energies.

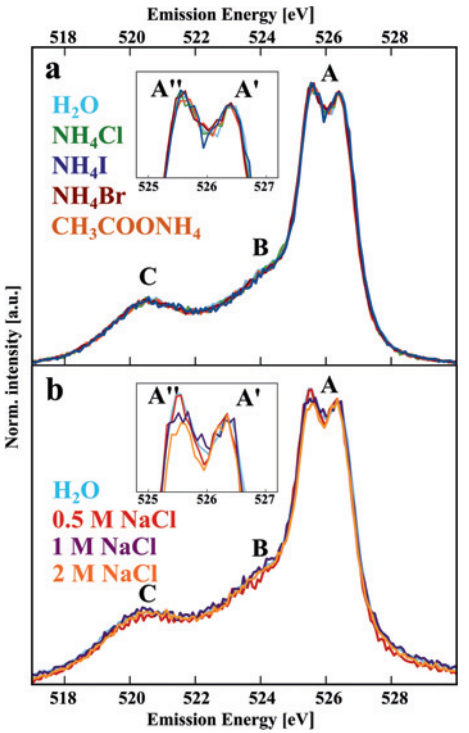

Figure 3: a) X-ray emission spectra for pure water and 500 mM ammonium solutions with changing anions. b) XE spectra for different concentration of NaCl. Significant structural changes are not observed for low salt concentration. For concentrations of 1 M and higher the A″ peak is lower compared to water.

of water has been proposed to be sensitive to the local hydrogen bond environment [21, 22]. The origin of the fine structure at peak A is still under discussion with commonly two models explaining this effect [21, 22, 43, 44]. Model (i) is assigning the origin due to two different structure motifs, denoted as high and low density of water, where peak A'' is due to tetrahedral coordinated water molecules with four intact hydrogen bonds and peak A' from distorted water configurations. In this model, the splitting is intrinsically caused by different 1s core levels between two structural motifs [22]. Model (ii) assigns the fine structure to a dynamical nuclear effect during the core-hole lifetime. While a core electron is promoted, the core hole has a certain lifetime, for oxygen in water this is around 4 fs. In this short time scale nuclear motion can occur. Peak A'' is from heterolytic dissociated water molecules and peak A' from intact water [21, 43, 44]. Both models have been challenged and supported with recent experiments, yet no consensus has been reached over the nature of the splitting [14–20, 23, 45].

There is consensus that the splitting is sensitive to the local hydrogen bond environment [21, 22]. Both models predict that peak A'' is sensitive to intact and peak A' to broken hydrogen bonds. Within these models, changes in the intensities of the lone pair electrons are anticipated. Depending on what characteristics these salts have, they are supposed to have different impact on the water molecules. Based on viscosity measurements, the anions studied have to enhance order or disorder of the hydrogen bond network [36, 37]. Yet, no impact is mirrored in the spectra. The question is why no significant changes are observed in the low concentrated salt solution spectra. With 500 mM only a small fraction of water molecules are in direct contact with the salt ions and most water molecules are bulk water. So the spectra are dominated by the fluorescence of bulk water. The opposite effect of cations and anions leading to compensation might also be a plausible explanation for the lack of changes. The NH_4^+ ion is characterized from viscosity experiments as a structure breaker and CH_3COO^- ion as a structure maker [36]. But this approach cannot explain why for structure breaker anions like I^- and Br^- no effect is observable [37]. In case of the Cl^- ion, recent results showed no impact on the hydrogen bond network [5, 9, 46].

Figure 3b shows a concentration measurement of aqueous NaCl solution with 500 mM, 1 M and 2 M.

Interestingly, significant changes are occurring for a concentration of 1 M or higher. The left peak A'' is decreasing with increasing salt concentrations. A qualitative interpretation within the (i) model means that the salt ion is reducing the number of tetrahedral coordinated water molecules. While the (ii) model is suggesting that the number of heterolytic dissociations decreases. Both interpretations lead to a reduction of intact hydrogen bonds. To estimate the magnitude of changes caused by the presence of salt ions the data have been quantitatively

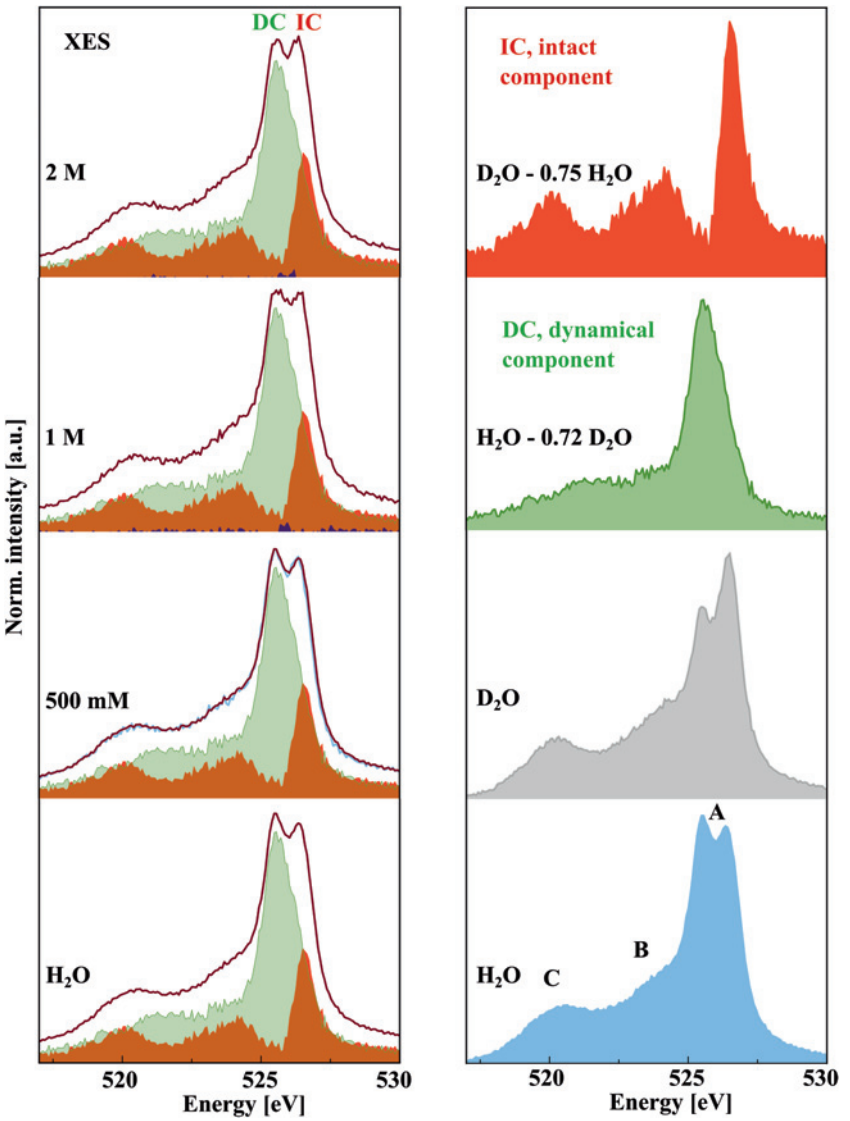

Figure 4: Left: The emission spectra for water and different $NaCl$ concentration are shown. A two component fit has been applied to reproduce the spectra of H_2O and the $500\,mM$ solution, while for the $1\,M$ and $2\,M$ salt solution an additional residue (dark blue) was necessary. The resulting fits as well as the components are color coded according to the right plot. The blue part illustrates the residue. Right: The X-ray emission spectra are shown for pure H_2O and D_2O on the oxygen edge. The components DC and IC were derived from the differences of H_2O and D_2O with weighting so negative values are avoided and the residues are the difference of the salt spectra and the two components fit.

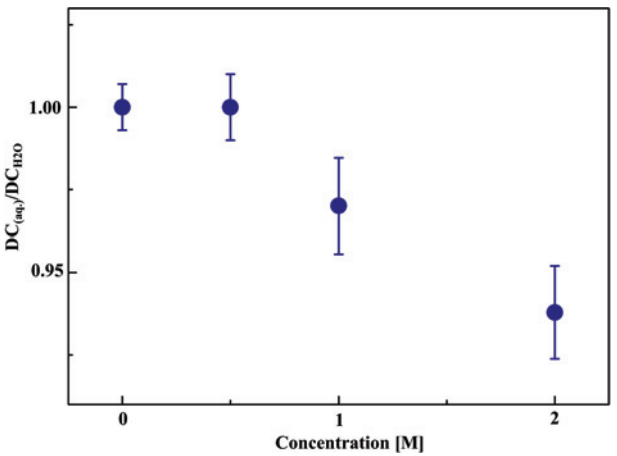

Figure 5: The relative ratio of $DC_{(aqu.)}/DC_{H_2O}$ in dependence of the salt concentration.

analyzed within the dynamic model (ii) using a superposition of several contributions [21], see Figs. 4 and 5. Figure 4 is also showing the X-ray emission spectrum of H_2O and D_2O on the oxygen edge. The emission spectrum of D_2O exhibits a strong isotope effect. The lower energy peak A″ is much more reduced for D_2O than for H_2O. It has been interpreted as an indication for the dynamic model, since the nuclear dynamics is suppressed compared to pure H_2O. Within the dynamical model the D_2O and H_2O emission spectra can be reproduced by a sum of dynamic (DC) and intact components (IC) [21]. The dynamic and the intact component were derived from the difference of H_2O with D_2O and vice versa with calculated weighting so there are no negative values.

The intact component spectrum resembles the X-ray emission signal of gas phase water with three well defined peaks, see Figure 1. While the dynamic component spectrum matches the signal of OH^-. A splitting has not been observed for water in gas phase for non-resonant excitation energies [20]. With different IC/DC ratio, the H_2O and D_2O signal can be recreated with 0.72 for H_2O and 1.33 for D_2O. This approach has been applied to the results from the concentration measurement since with higher concentration the lower energy peak is decreasing. The results and the fit with the single components is illustrated color coded in Figure 4. The IC/DC ratio increases from 0.72 for H_2O to 0.78 for 1 M up to 0.83 for 2 M salt solution. The ration for the 500 mM equals the value for water. The increase of the ratio is mainly due to a reduction of the dynamical component meaning that the contribution of heterolytic dissociated water molecules is decreasing with higher salt concentrations. A similar behavior with temperature dependent study has been observed by Fuchs et al. [21], where the intensity of peak A″ is diminishing with higher temperature confirming the reduction

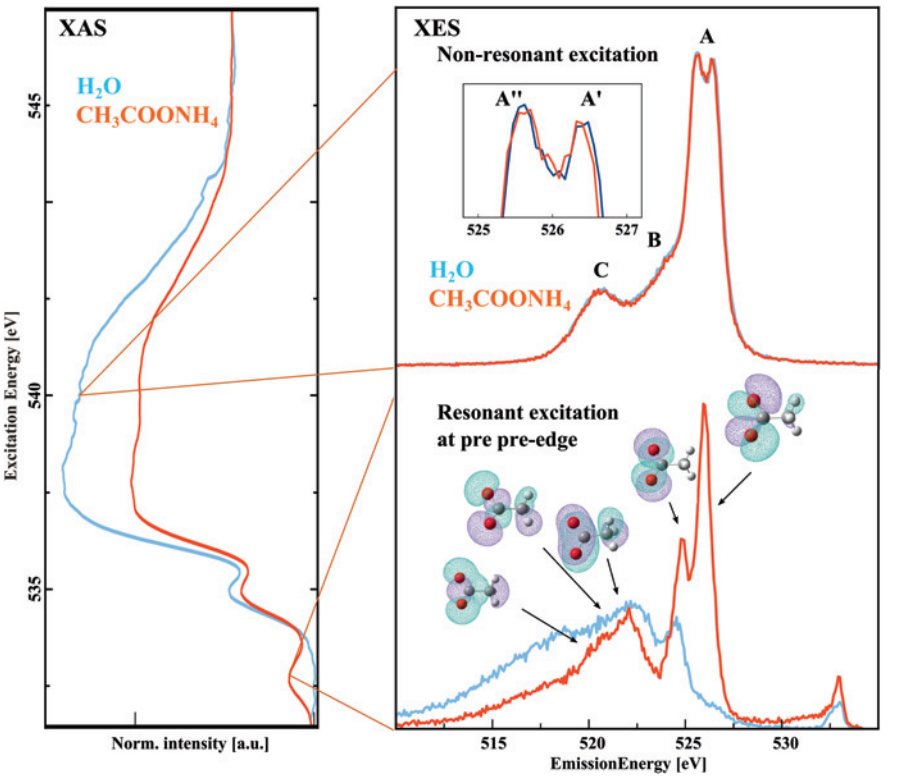

Figure 6: The X-ray absorption and emission spectra of oxygens of the CH_3COO^- and water show significant structural differences. While the non-resonant spectra show negligible changes, at resonant excitation energy of the oxygen edge of CH_3COO^- essentially oxygen from the anion is probed.

of intact hydrogen bonds. For the 1 and 2 M spectra, a residue is introduced as a difference between the measured data and the two component fit. It has been proposed that the residue can be interpreted as being the signal from the water molecules in the first solvation shell of the salt ion [16]. Yet, the residues are not significant, which could be due to insufficient signal from water molecules in the first solvation shell. Figure 5 is displaying how much the part of the dynamic component is decreasing with higher concentration. The dynamic component is reduced by approx. $6.3 \pm 1.4\%$ for the 2 M salt solution. The high concentration spectrum suggests that Na^+ ions decrease the number of intact hydrogen bonds and cause more disorder [5]. Since changes seem to be dependent on the concentration, it indicates a local impact of Na^+. This finding is in agreement with recent results [5, 16, 33, 34].

It is intriguing that the oxygens from CH_3COO^- ions don't contribute to the XE signal significantly see Figure 3.

Figure 6 displays the XAS of pure water and 2 M ammonium acetate solution measured in transmission mode and the XE spectra of water and 500 mM CH_3COONH_4 solution at two different excitation energies.

The XA spectra show the characteristics water features, namely the pre-edge (~ 535 eV), the main-edge (~ 538 eV) and the post-edge (~ 540 eV) as reported by previous studies [7, 11, 12, 39].

The higher concentration for XAS measurement has been used to emphasize the feature around 533 eV before the pre edge of water at 535 eV. A 500 mM solution has also been measured and shows the same effect with less intensity.

The XA spectrum of the salt solution seems saturated. The saturation affects greatly the pre- to main-edge ratio due to a suppression of the main edge. Since the XA measurements were carried out using a transmission cell, the sources for the saturation effect could be due to sample thickness greater than 600 nm or/and inhomogeneity of the sample thickness within the beam spot [39]. However, the pre pre-edge feature is not caused by saturation effects.

The absorption peak around 533 eV is clearly a signal from the oxygens from CH_3COO^- ion and is specific to the carboxylate group since at that energy there is absent absorption of oxygen in water.

The different absorption edges of water and acetate are due to different bonding characteristics. In detail, the pre pre-edge peak is assigned to the $O_{C=O}(\pi^* \leftarrow 1s)$ transition [47, 48]. The emission signal at resonant excitiation energy is mainly from the anion. It shows two sharp peaks around 525 eV and 526 eV, which can be assigned to in plane and out of plane lone pair orbitals. The other emission peaks between 520 eV and 523 eV are from bonding orbitals of the methyl group. As comparison, a pure water spectrum is shown in Figure 4 at that excitation energy. So it is possible to probe the sample in a site specific way and extract site sensitive information. Interesting though is the lack of changes for non-resonant excitation energy. The overall emission signal is dominated by bulk water molecules. The lack of contribution of oxygen from CH_3COO^- can also be due to much lower cross section for non-resonant excitation energies. This approach has been utilized to study ion-ion pairing and anion-water interaction [9]. The monochromatic character of lightsources allows the possibility to probe element and site specifically and extract information about the interaction with the chemical environment.

4 Summary

We have performed XAS, XES and RIXS experiments on water and various salt solutions with different anions on the oxygen K-edge in combination with the liquid jet and the liquid cell. All non-resonant excited data show a multi peak structure in the lone pair regime. We could show how salt ions can change the hydrogen bond structure and how it is monitored in the electronic configuration. The concentration measurements indicate that only water molecules in close proximity of the ion are affected and no long range impact of Na^+ could be monitored.

Additionally, we showed the possibility to use RIXS as a method to probe systems in a site specific way. X-ray spectroscopy coupled with the liquid jet opens a door to a new series of experiments to study the local charge distributions of biochemical systems in the liquid phase.

Acknowledgement: We thank the beamline staff at U41_PGM, U49-2_PGM_1 of HZB and P04 of PETRA III. This work was supported by SFB755 "Nanoscale Photonic Imaging" and SFB 1073 "Atomic Scale Control of Energy Conversion" of the German Science Foundation (DFG), the Advanced Study Group of the Max Planck Society, Deutsches Elektronen-Synchrotron, Helmholtz Zentrum Berlin and Helmholtz Virtual Institute "Dynamic Pathways in Multidimensional Landscapes". H. F., S. W. and K. U. are grateful for support from the X-ray Free Electron Laser Priority Strategy Program of MEXT. We thank B. Winter and L. Weinhardt for valuable discussions.

References

1. L. Ament, M. van Veenendaal, T. Devereaux, J. Hill, and J. van den Brink, Rev. Mod. Phys. **83** (2011) 705.
2. B. Winter and M. Faubel, Chem. Rev. **106** (2006) 1176.
3. A. Nilsson, D. Nordlund, I. Waluyo, N. Huang, H. Ogasawara, S. Kaya, U. Bergmann, L.-Å. Näslund, H. Öström, P. Wernet, K. J. Andersson, T. Schiros, and L. G. M. Pettersson, J. Electron Spectrosc. **177** (2010) 99.
4. F. Gel'mukhanov and H. Agren, Phys. Rev. A **56** (1997) 2676.
5. Z. Yin, I. Rajkovic, K. Kubicek, W. Quevedo, A. Pietzsch, P. Wernet, A. Föhlisch, and S. Techert, J. Phys. Chem. B **118** (2014) 9398.
6. L. Weinhardt, M. Blum, O. Fuchs, A. Benkert, F. Meyer, M. Bär, J. D. Denlinger, W. Yang, F. Reinert, and C. Heske, J. Electron Spectrosc. **188** (2013) 111.
7. P. Wernet, D. Nordlund, U. Bergmann, M. Cavalleri, M. Odelius, H. Ogasawara, L. A. Näslund, T. K. Hirsch, L. Ojamäe, P. Glatzel, L. G. M. Pettersson, and A. Nilsson, Science **304** (2004) 995.

8. P. Wernet, K. Kunnus, S. Schreck, W. Quevedo, R. Kurian, S. Techert, F. M. F. De Groot, M. Odelius, and A. Föhlisch, J. Phys. Chem. Lett. **3** (2012) 3448.
9. T. Petit, K. M. Lange, G. Conrad, K. Yamamoto, C. Schwanke, K. F. Hodeck, M. Dantz, T. Brandenburg, E. Suljoti, and E. F. Aziz, Struct. Dyn. **1** (2014) 034901.
10. K. M. Lange, R. Könnecke, M. Soldatov, R. Golnak, J.-E. Rubensson, A. Soldatov, and E. F. Aziz, Angew. Chem. **123** (2011) 10809.
11. C. D. Cappa, J. D. Smith, B. M. Messer, R. C. Cohen, and R. J. Saykally, J. Phys. Chem. B **110** (2006) 5301.
12. L.-A. Näslund, D. C. Edwards, P. Wernet, U. Bergmann, H. Ogasawara, L. G. M. Pettersson, S. Myneni, and A. Nilsson, J. Phys. Chem. A **109** (2005) 5995.
13. K. Kunnus, I. Josefsson, S. Schreck, W. Quevedo, P. S. Miedema, S. Techert, F. M. F. De Groot, M. Odelius, P. Wernet, and A. Föhlisch, J. Phys. Chem. B **117,** 16512 (2013).
14. S. Schreck, A. Pietzsch, K. Kunnus, B. Kennedy, W. Quevedo, P. S. Miedema, P. Wernet, and A. Föhlisch, Struct. Dyn. **1** (2014) 054901.
15. A. Pietzsch, F. Hennies, P. S. Miedema, B. Kennedy, J. Schlappa, T. Schmitt, V. N. Strocov, and A. Föhlisch, Phys. Rev. Lett. **114** (2015) 088302.
16. Y. L. Jeyachandran, F. Meyer, S. Nagarajan, A. Benkert, M. Bär, M. Blum, W. Yang, F. Reinert, C. Heske, L. Weinhardt, and M. Zharnikov, J. Phys. Chem. Lett. **5** (2014) 4143.
17. Y. Harada, T. Tokushima, Y. Horikawa, O. Takahashi, H. Niwa, M. Kobayashi, M. Oshima, Y. Senba, H. Ohashi, K. T. Wikfeldt, A. Nilsson, L. G. M. Pettersson, and S. Shin, Phys. Rev. Lett. **111** (2013) 193001.
18. J. A. Sellberg, T. A. McQueen, H. Laksmono, S. Schreck, M. Beye, D. P. DePonte, B. Kennedy, D. Nordlund, R. G. Sierra, D. Schlesinger, T. Tokushima, I. Zhovtobriukh, S. Eckert, V. H. Segtnan, H. Ogasawara, K. Kubicek, S. Techert, U. Bergmann, G. L. Dakovski, W. F. Schlotter, Y. Harada, M. J. Bogan, P. Wernet, A. Föhlisch, L. G. M. Pettersson, and A. Nilsson, J. Chem. Phys. **142** (2015) 044505.
19. J. Forsberg, J. Gråsjö, B. Brena, J. Nordgren, L.-C. Duda, and J.-E. Rubensson, Phys. Rev. B **79** (2009) 1.
20. L. Weinhardt, A. Benkert, F. Meyer, M. Blum, R. G. Wilks, W. Yang, M. Bär, F. Reinert, and C. Heske, J. Chem. Phys. **136** (2012) 144311.
21. O. Fuchs, M. Zharnikov, L. Weinhardt, M. Blum, M. Weigand, Y. Zubavichus, M. Bär, F. Maier, J. Denlinger, C. Heske, M. Grunze, and E. Umbach, Phys. Rev. Lett. **100** (2008) 027801.
22. T. Tokushima, Y. Harada, O. Takahashi, Y. Senba, H. Ohashi, L. G. M. Pettersson, A. Nilsson, and S. Shin, Chem. Phys. Lett. **460** (2008) 387.
23. T. Tokushima, Y. Horikawa, H. Arai, Y. Harada, O. Takahashi, L. G. M. Pettersson, A. Nilsson, and S. Shin, J. Chem. Phys. **136** (2012) 0445171.
24. M. Faubel, S. Schlemmer, and J. P. Tönnies, Z. Phy. D, Atom. Mol. Cl. **10** (1988) 269.
25. Y. Zhang and P. S. Cremer, Curr. Opin. Chem. Biol. **10** (2006) 658.
26. P. Lo Nostro and B. W. Ninham, Chem. Rev. **112** (2012) 2286.
27. P. Jungwirth and D. J. Tobias, Chem. Rev. **106** (2006) 1259.
28. M. U. Sander, K. Luther, and J. Troe, Ber. Bunsen. Phys. Chem. **97** (1993) 953.
29. M. U. Sander, K. Luther, and J. Troe, J. Phys. Chem. **97** (1993) 11489.
30. M. U. Sander, M. S. Gudiksen, K. Luther and J. Troe, Chem. Phys. **258** (2000) 257.
31. E. Vöhringer-Martinez, B. Hansmann, H. Hernandez, J. S. Francisco, J. Troe, and B. Abel, Science **315** (2007) 497.
32. H. J. Bakker, Chem. Rev. **108** (2008) 1456.

33. A. W. Omta, M. F. Kropman, S. Woutersen, and H. J. Bakker, Science **301** (2003) 347.
34. R. Mancinelli, A. Botti, F. Bruni, M. A. Ricci, and A. K. Soper, J. Phys. Chem. B **111** (2007) 13570.
35. K. J. Tielrooij, N. Garcia-Araez, M. Bonn, and H. J. Bakker, Science **328** (2010) 1006.
36. H. D. B. Jenkins and Y. Marcus, Chem. Rev. **95** (1995) 2695.
37. Y. Marcus, Pure Appl. Chem. **82** (2010) 1889.
38. K. Kunnus, I. Rajkovic, S. Schreck, W. Quevedo, S. Eckert, M. Beye, E. Suljoti, C. Weniger, C. Kalus, S. Grübel, M. Scholz, D. Nordlund, W. Zhang, R. W. Hartsock, K. J. Gaffney, W. F. Schlotter, J. J. Turner, B. Kennedy, F. Hennies, S. Techert, P. Wernet, and A. Föhlisch, Rev. Sci. Instrum. **83** (2012) 123109.
39. S. Schreck, G. Gavrila, C. Weniger, and P. Wernet, Rev. Sci. Instrum. **82** (2011) 103101.
40. I. Rajkovic, J. Hallmann, S. Grübel, R. More, W. Quevedo, M. Petri, and S. Techert, Rev. Sci. Instrum. **81** (2010) 0451051.
41. C. Weber, Z. Angew. Math. Mech. **11** (1931) 136.
42. M. Goldin, J. Yerushal, R. Pfeffer, and R. Shinnar, J. Fluid Mech. **38** (1969) 689.
43. M. Odelius, Phys. Rev. B **79** (2009) 144204.
44. M. Odelius, J. Phys. Chem. A **113** (2009) 8176.
45. K. Nishizawa, N. Kurahashi, K. Sekiguchi, T. Mizuno, Y. Ogi, T. Horio, M. Oura, N. Kosugi, and T. Suzuki, Phys. Chem. Chem. Phys. **13** (2011) 413.
46. H. J. Kulik, N. Marzari, A. A. Correa, D. Prendergast, E. Schwegler, and G. Galli, J. Phys. Chem. B **114** (2010) 9594.
47. T. Tokushima, Y. Horikawa, Y. Harada, O. Takahashi, A. Hiraya, and S. Shin, Phys. Chem. Chem. Phys. **11** (2009) 1679.
48. Y. Horikawa, T. Tokushima, Y. Harada, O. Takahashi, A. Chainani, Y. Senba, H. Ohashi, A. Hiraya, and S. Shin, Phys. Chem. Chem. Phys. **11** (2009) 8676.